Dependence of peak gain on pump wavelength, pump power, numerical aperture and doping concentration of silica-based thulium doped fiber amplifier (TDFA) for 2µm region

CHAHAT GUPTA[1], RAJANDEEP SINGH[1,*], RAMANDEEP KAUR[2], GURPREET KAUR[3]
[1]*Guru Nanak Dev University, Amritsar, India*
[2]*Punjabi University, Patiala, India*
[3]*Chandigarh University, Mohali, India*

In this paper dependence of peak gain of TDFA on the pump power is investigated. Here, four pumps of wavelength 1050 nm, 1560 nm, 1700 nm, 1740 nm have been used individually. The numerical aperture values of 0.3 and 0.4 for each pump wavelength have been considered. Also, ion densities of 15.6×10^{24} m^{-3}, 20×10^{24} m^{-3}, 30×10^{24} m^{-3}, 40×10^{24} m^{-3} are set for each pump wavelength. A varied pump power from 20 mW to 300 mW has been used. In this way, eight simulation cases have been carried out for each pumping scheme and the gain curves are plotted to check the dependence of peak gain on pump power. It has been observed that the numerical aperture 0.4 gives better gain as compared to 0.3 in every pumping case. It is found that as the pump power increases, peak gain also increases. The peak gain is obtained at 1830 nm wavelength in each pumping case. For pump power 300 mW, the maximum peak gain of 19.4dB has been found for 1050 nm pump. The peak gain values found in the cases of the 1560 nm, 1700 nm and 1740 nm pumps are 33.39dB, 34.088dB, 34.34dB, respectively.

(Received September 15, 2021; accepted February 10, 2022)

Keywords: TDFA, Silica, Gain, Doping concentration, Pump power

1. Introduction

There is an exponential increase in traffic in telecommunication networks over the past few decades [1]. Erbium doped fiber amplifier (EDFA) is the most used optical amplifier because of the gain in the low loss C-band [2]. New approaches to data transmission are motivating to increase the transmission capacity beyond C-band [3]. The region of 2 µm wavelength is acquiring attractive attention for data transmission due to several reasons. First, hollow-core photonic band-gap fibers (transmission medium) provide a low loss window in this spectral region. Secondly, thulium doped fiber amplifiers (TDFAs) are being used for optical communication, giving low noise amplification and high gain in the 2µm region. Moreover, $^3F_4$,$^3H_6$ transition covers about 1700-2100 nm bandwidth of amplification [4]. This bandwidth coverage is two times more than Erbium doped fiber amplifier (EDFA) with the same configuration and complexity [5]. Silica-based TDFAs are easy to splice with the standard single-mode fibre, these are non-toxic in nature and their manufacturing is easy [6]. The Fluoride TDFA lacks these qualities. However, the phonon energy is higher in silica TDFA which results in poor efficiency and lower gain [7], [8]. TDFA is in use for the S-band as it is the only established rare-earth-doped fiber of this band [8], [9]. Apart from the S-band, the TDFA has a significant gain region in the 2µm region. A detailed mathematical model of the TDFA behaviour with a 1064 nm pump was presented by P. Peterka et al. [10]. In silica-based TDFA, the gain can be improved by analyzing the effect of various parameters. In literature, silica-based TDFAs with various pumping techniques have been presented. The Tm-doped fiber can be described in terms of rate and propagation equations in accord with the thulium energy level diagram shown in Fig. 1 [10].

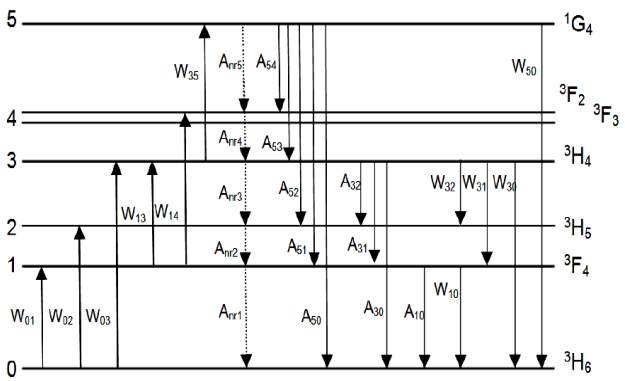

Fig. 1. Tm energy level diagram [10].

Due to their proximity, levels $^3F_2$ and $^3F_3$ are treated as a single level. The rate equations account for the spectral bands of 800 nm, 1470 nm and 1800 nm. Also, the

rate equations describe the effects of absorption, stimulated emission, and spontaneous emission on the populations of levels 0, 1, 3, and 5 (since nonradiative decay rates from levels 4 and 2 to the underlying level are high, the population of both levels are neglected in the model).

For the relevant levels N0, N1, N3, and N5, the rate equations are given by P. Peterka et al. [10].

$\frac{dN1}{dt}$=$N0.(W01+W02)-N1.(W10+W13+W14+Anr1+A10)$
$+N3.(W31+W32+Anr3+A32)+N5.(A51+A52)$
$\frac{dN3}{dt}$=$N0.(W03)+N1.(W13+W14)-N3.(W35+W32+W31+$
$W30+Anr1+A32+A31+A30)+N5.(Anr5+A54+A53)$
$\frac{dN5}{dt}$=$N0.(W05)+N3.(W35)-N5.(W50+Anr5+A54+A53+A$
$52+A50)$
and Nt=N0+N1+N3+N5

where N0, N1, N3, N5 and Nt are the population density of $^3H_6$,$^3F_4$,$^3H_4$,$^1G_4$ and total electron density respectively, Wij is the stimulated absorption and emission rates from i level to j level. Aij and Anrj are the radiative and non-radiative decay rates respectively. Assuming that the thulium ions are excited homogeneously across the fiber cross-section, the transition rates Wij can be defined by

$$Wij\ (z)= \int_0^{\infty} \frac{\sigma v(v)}{h.v} .I(z,v).dv \text{ [10]}$$

where $I(z,v)=i(r,\emptyset,v).Pk(z)$, h is Planck's constant, v is the frequency, σv is the transition cross-section and I is the light intensity distribution. The normalized optical intensity is defined by and Pk is the power of the kth beam.

The normalized optical intensity is defined as Pk for the kth beam [10].

$$\frac{dP_k}{dz} =$$
$$u_k.P_k(z).\sum_{ij}^{(10,30,31.50)} \int_0^{2\pi} \int_0^{\infty} \left(\sigma_{ij}(v_k).N_i(r,\emptyset,z) - \sigma_{ji}(v_k).N_j(r,\emptyset,z)\right).i_k(r,\emptyset).r.dr.d\emptyset -$$
$$u_k.P_k(z).\sum_{ij}^{(02,14,35)} \int_0^{2\pi} \int_0^{\infty} \left(\sigma_{ji}(v_k).N_i(r,\emptyset,z)\right).i_k(r,\emptyset).r.dr.d\emptyset +$$
$$u_k.P_{0k}\sum_{ij}^{(10,30,31.50)} \int_0^{2\pi} \int_0^{\infty} \left(\sigma_{ij}(v_k).N_i(r,\emptyset,z).i_k(r,\emptyset).r.dr.d\emptyset - \alpha(v_k).u_k.P_k(z)\right)$$

where for forward propagating waves uk is +1 and it is -1 for backward propagating waves, P_{0k} means the spontaneous emission contribution from the local population Ni. The propagation equation [10] of the beams through the doped fiber is given by

$$\frac{dP^+(\lambda)}{dz} =$$
$$\Gamma(\lambda).P^+(\lambda).\sum_{ij}^{(10,30,31.50,32)} \left(N_i.\sigma_{ij}(\lambda).-N_j.\sigma_{ij}(\lambda)\right) -$$
$$\Gamma(\lambda).P^+(\lambda).\left(N_0.\sigma_{02}(\lambda) + N_1\sigma_{14}(\lambda) + N_3\sigma_{35}(\lambda)\right) +$$
$$\Gamma(\lambda).\sum_{ij}^{(10,30,31,50,32)} 2hv_{ij}\Delta v\, N_i.\sigma_{ij}(\lambda) - \alpha(\lambda).P^+(\lambda)$$

By setting the time derivatives $\frac{dN1}{dt}$, $\frac{dN3}{dt}$, $\frac{dN5}{dt}$ to zero, the problem reduces to the steady-state case. With the specified boundary conditions at z = 0 and z = L the equations are integrated over space, and frequency, from the input power and output power, the gain is obtained [8], [10], [11]. The Optisystem 13 has been used for simulations. Fig. 2 shows the detailed energy level diagram of thulium ions in the 2µm region with pumping schemes. The gain of TDFA depends upon the population inversion and population density at different energy levels. To achieve high gain, the lower level must be depopulated, therefore a pump is used. $^3F_4$ to $^3H_6$ transition in Tm ion covers about 1700 to 2100 nm. Thulium ions show strong ground-state absorption (GSA: $^3H_6$ to $^3F_4$) using a pumping scheme. This leads to population inversion between $^3H_6 \rightarrow {}^3F_4$. Ions at $^3F_4$ level emit a photon and drop to the $^3H_6$ level. This process is repeated again and again. This leads to population inversion and then amplification [12].

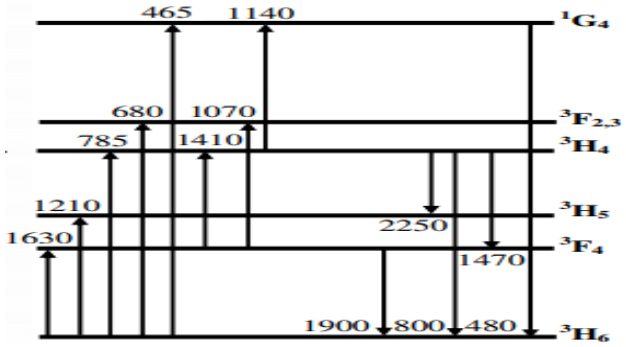

Fig. 2. Detailed Tm energy level diagram for 2µm region with pumping schemes [12]

2. System setup

Fig. 3 shows the system setup used in this paper. A continuous-wave laser array consisting of 50 laser inputs, each having -20dB power is used, the signal power is kept at -20dB as the present analysis is for small signal amplification. The wavelengths from 1750 nm to 2240 nm with channel spacing of 10 nm have been assigned to the lasers. All the wavelengths are multiplexed together with the help of MUX and then fed to the pump coupler. In the coupler, the pump is combined with the signals. Power in each pumping case has been varied from 20 mW to 300 mW. The pumps used are 1050 nm, 1560 nm, 1700 nm and 1740 nm in separate cases. The combined signal is then fed to the silica-based thulium doped fiber. The length of TDF is fixed to 10 m, core radius to 1.3 µm, doping radius to 1.3 µm. Then results can be taken using a dual-port WDM analyser

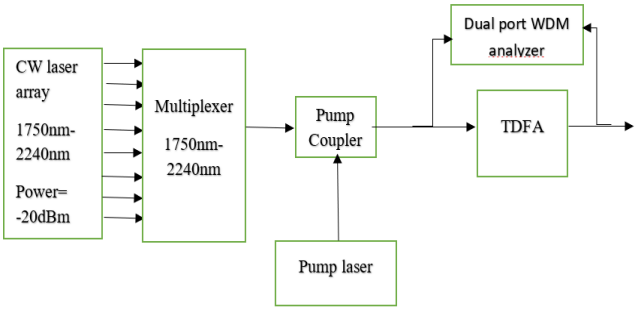

Fig. 3. System setup

In this paper, the numerical aperture value of 0.3, 0.4 and thulium ion density of 15.6×10^{24} m^{-3}, 20×10^{24} m^{-3}, 30×10^{24} m^{-3}, 40×10^{24} m^{-3} has been used for each pump. The pump power is varied from 20 mW to 300 mW. The effect of doping concentration, pumping wavelength, numerical aperture and pump power on the peak gain is investigated in this paper. The graphs between pump power and peak gain have been plotted using Matlab and the simulations are carried out using Optisystem 13. The parameters of TDFA and pumping scenarios used in the simulation are shown in Table 1.

Table 1. Parameters of TDFA

Parameter	Value
Length of TDF	10 m
Pump Wavelength	1050 nm,1560 nm,1700 nm, 1740 nm
Doping concentration	15.6×10^{24} m^{-3}, 20×10^{24} m^{-3}, 30×10^{24} m^{-3}, 40×10^{24} m^{-3}
Pump Power	20 mW-300 mW
Core radius of TDF	1.3 um
Doping radius of TDF	1.3 um
Numerical Aperture	0.3, 0.4

3. Results and discussion

The results are divided into four parts. The first part shows results for a pump wavelength of 1050 nm with both numerical aperture and all doping concentration values. Similarly, the second part shows results for the pump wavelength of 1560 nm. In the third part results for the pump wavelength of 1700 nm have been shown. Then the results for a pump wavelength of 1740 nm have been shown.

A. For pump wavelength 1050nm

Fig. 4 shows the gain and noise figure variation wrt the signal wavelength. In this case, the doping concentration of 15.6×10^{24} m^3 and the numerical aperture of 0.3 is set. It can be clearly visualized that the gain for all wavelengths increases with an increase in pump power. The peak gain for every pump power has been observed at the signal wavelength of 1830 nm. Gain values at all the other wavelengths are proportional to the peak gain. It can be concluded that by maximizing peak gain, the gain for all the signal wavelengths can be improved.

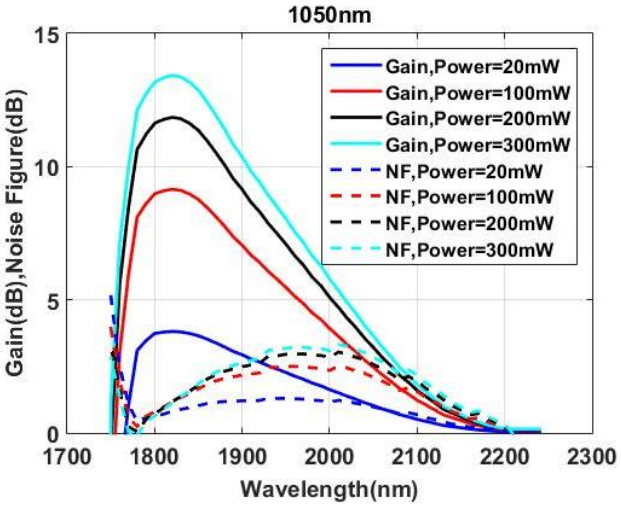

Fig. 4. Gain vs. Wavelength for 1050 nm pump (color online)

Also, the noise figure variation has been shown in Fig. 4. The noise figure is very low in the region where TDFA is providing a significant gain, noise figure peaks near 2000 nm wavelength. The value of the noise figure remains less than 4 dB which is quite low. Therefore, in Fig. 5 the analysis of peak gain variation as a function of pump power is carried out for eight different sets of combinations of numerical apertures and doping concentrations.

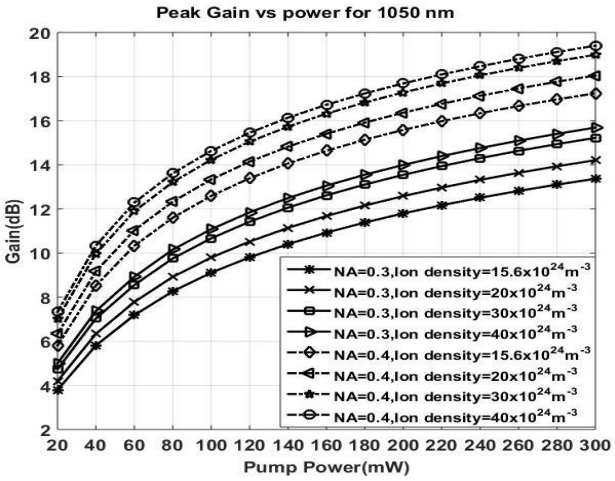

Fig. 5. Peak gain at 1830 nm for 1050 nm pump for pump power 20 mW-300 mW

It can be seen that the highest peak gain is obtained for pump power 300 mW and minimum peak gain is obtained for pump power 20 mW in each of the eight cases. The observed values of the gain for pump power 300 mW and NA-0.3 are 13.37dB, 14.21dB, 15.22dB and 15.69dB for doping concentrations of 15.6×10^{24} m^{-3}, 20×10^{24} m^{-3}, 30×10^{24} m^{-3}, 40×10^{24} m^{-3} respectively. Also, the values of gain for pump power 300mW, NA-0.4 are 17.24dB, 18.05dB, 18.99dB and 19.40dB for doping concentration 15.6×10^{24} m^{-3}, 20×10^{24} m^{-3}, 30×10^{24} m^{-3}, 40×10^{24} m^{-3} respectively. Gain for NA- 0.4 is better than NA-0.3 in each case.

B. For pump wavelength 1560 nm

Fig. 6 shows the gain and noise figure for the input wavelength range of 1740 nm to 2240 nm when a pump of 1560 nm is used. In this case, the results have been shown for the numerical aperture of 0.3 and doping concentration of 15.6×10^{24} m^3. In this case, the gain at 1740 nm is zero but the gain increases when the wavelength increases to 1830 nm. The gain increases with the increase in pump power for all pump cases. The gain is maximum at 1830 nm in each pumping case.

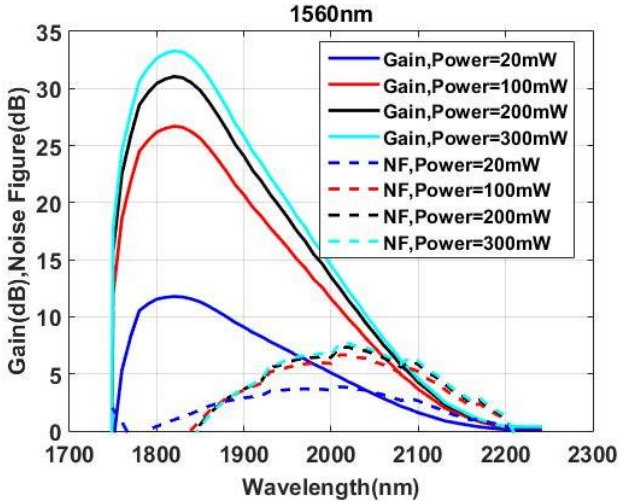

Fig. 6. Gain vs. Wavelength for 1560 nm pump (color online)

The noise figure is also shown in Fig. 6, the noise figure, in this case, is similar to the case of 1050 nm pumping. The noise figure is very low in the region where the gain of TDFA is high. The noise figure in all the cases is less than 7 dB, the noise figure is highest in case of highest pump power.

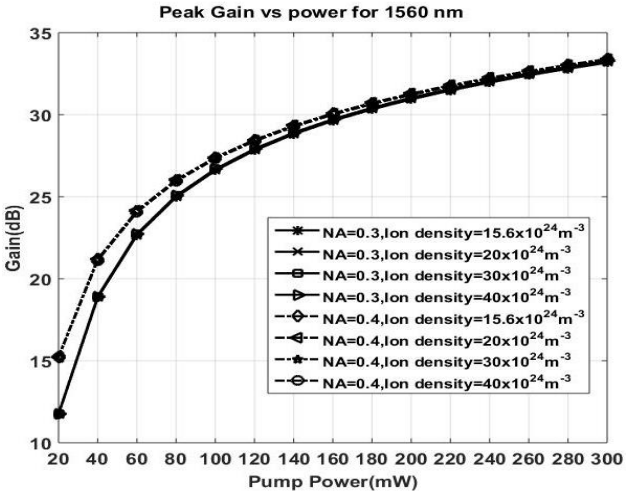

Fig. 7. Peak gain at 1830 nm for 1560 nm pump for pump power 20 mW-300 mW

Fig. 7 shows the results for all the eight combinations taken for pump wavelength 1560 nm. It can be considered that the first four cases are overlapping and the last four cases are overlapping. Also, the highest peak gain is obtained for pump power 300 mW and the minimum peak gain is obtained for pump power 20 mW in each of the eight cases. The values of the gain for pump power 300 mW and NA- 0.3 are 33.17dB, 33.22dB, 33.27dB, and 33.28dB for doping concentrations of 15.6×10^{24} m^{-3}, 20×10^{24} m^{-3}, 30×10^{24} m^{-3}, 40×10^{24} m^{-3} respectively. Also, the values of gain for pump power 300 mW, NA-0.4 are 33.38dB, 33.40dB, 33.38dB and 33.33dB for doping concentrations of 15.6×10^{24} m^{-3}, 20×10^{24} m^{-3}, 30×10^{24} m^{-3}, 40×10^{24} m^{-3} respectively. Gain for the NA-0.4 is found better than NA-0.3 in every case. It is very clear from the above discussion that the difference between the gain values for NA-0.3 for all the pumping and doping cases is negligible. A similar trend is seen for the NA-0.4, in this, the gain is found independent from the pumping and doping cases.

C. For pump wavelength 1700 nm

Fig. 8 shows the gain and noise figure variation with respect to signal wavelength for different pump power values. It can be seen from the graph that the gain at all wavelengths is proportional to pump power, the gain increases as the pump power increases. In this case, the noise figure is again less than 7dB. The noise figure is less than 5 dB for wavelengths up to 1900 nm.

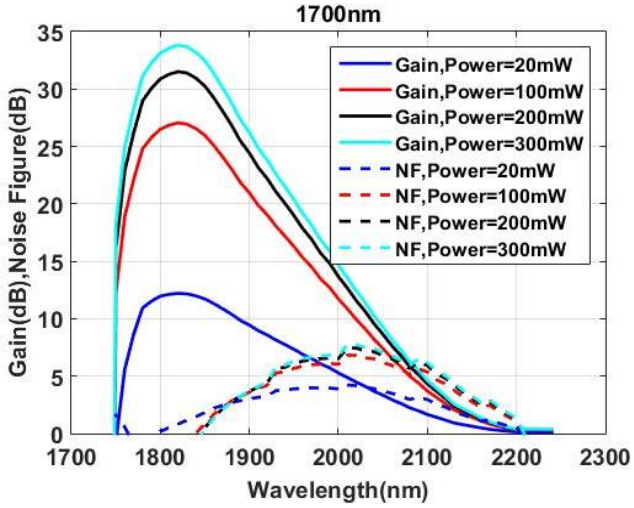

Fig. 8. Gain vs. Wavelength for 1700 nm pump

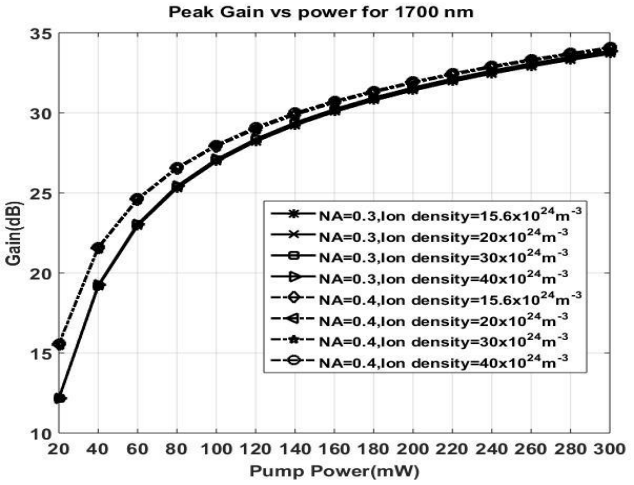

Fig. 9. Peak gain at 1830 nm for 1700 nm pump for pump power 20 mW-300 mW

Fig. 9 shows the results for all the eight combinations taken for pump wavelength 1700 nm. It is clear from the above graph that the first four cases are overlapping and the last four cases are overlapping. Also, the highest peak gain is obtained for pump power 300 mW and the minimum peak gain is obtained for pump power 20 mW in each of the eight cases. The values of the gain for pump power 300 mW and NA-0.3 are 33.68dB, 33.73dB, 33.82dB and 33.87dB for doping concentrations of 15.6×10^{24} m^{-3}, 20×10^{24} m^{-3}, 30×10^{24} m^{-3}, 40×10^{24} m^{-3} respectively. Also, the values of gain for pump power 300mW and NA-0.4 is 33.40dB, 34.03dB, 34.09dB and 34.09dB for doping concentrations of 15.6×10^{24} m^{-3}, 20×10^{24} m^{-3}, 30×10^{24} m^{-3}, 40×10^{24} m^{-3} respectively. The gain for NA-0.4 is found better than NA-0.3 in every considered case. It shows that the difference between the values of gain for NA-0.3 for all the cases is negligible and the same is true in the case for NA-0.4. For every considered case, the gain increase sharply as the pump power increases from 20 mW to 80 mW. Above 80 mW pump power, the slope of gain increases reduces as compared to the pump power lower than 80 mW.

D. For pump wavelength 1740 nm

Fig. 10 shows the gain variation in the pumping case of 1740 nm. In this case, the gain values for 200 mW pump power and 300 mW pump power are almost the same. The same trend can be seen from Fig. 11 looking at the curve for the concertation of 15.6×10^{24} m^{-3} and NA of 0.3. In this case, the increase in the pump from 200 mW to 300 mW is not improving the gain significantly. The noise figure values for this pumping case are very low the noise figure is always less than 5 dB for the entire band of input wavelengths.

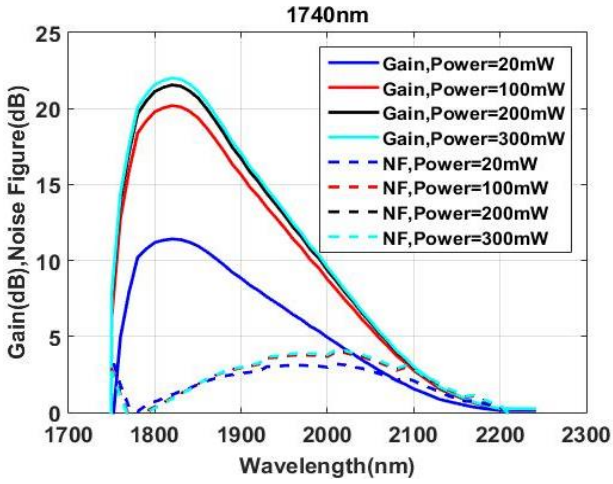

Fig. 10. Gain vs. Wavelength for 1740 nm pump

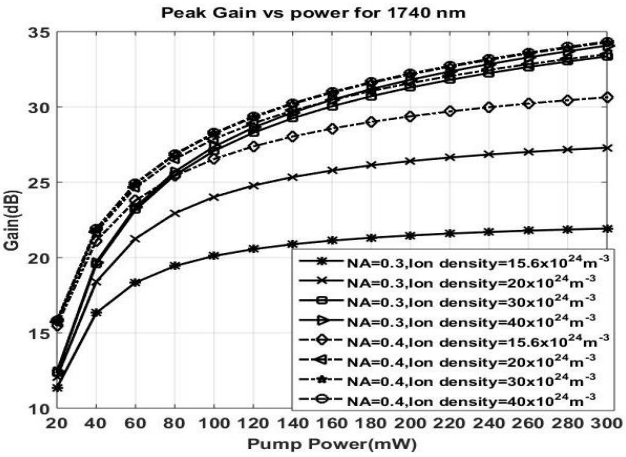

Fig. 11. Peak gain at 1830 nm for 1740 nm pump for pump power 20 mW-300 mW

Fig. 11 shows the results for all the eight combinations taken for pump wavelength 1740 nm. It can be seen that the highest peak gain is obtained for pump power 300 mW and minimum peak gain is obtained for pump power 20 mW in each of the eight cases. The values of gain for pump power 300 mW and NA- 0.3 are

21.93dB, 27.29dB, 33.35dB and 34.06dB for doping concentrations of 15.6×10^{24} m^{-3}, 20×10^{24} m^{-3}, 30×10^{24} m^{-3}, 40×10^{24} m^{-3} respectively. Also, the values of gain for pump power 300 mW and NA-0.4 are 30.64dB, 33.49dB, 34.28dB and 34.34dB for doping concentrations of 15.6×10^{24} m^{-3}, 20×10^{24} m^{-3}, 30×10^{24} m^{-3}, 40×10^{24} m^{-3} respectively. The gain for NA-0.4 is better than NA-0.3 in for every fixed pumping and doping case. For both NA-0.3 and NA-0.4, the gain increases as doping concentration increases from 15.6×10^{24} m^{-3} to 40×10^{24} m^{-3}.

E. Comparison of pumping cases

Fig. 12 shows the comparison of the pumping cases when the doping concentration of 15.6×10^{24} m^{-3} has been chosen. In this case, it can be seen the 1050 nm pump is the least efficient. The 1740 nm pump provides better gain as compared to the 1050 nm pump but gain saturates for pump power higher than 100 mW. The 1560 nm and 1700 nm pumps are showing almost the same performance, there is very little difference in the gain curves for these cases.

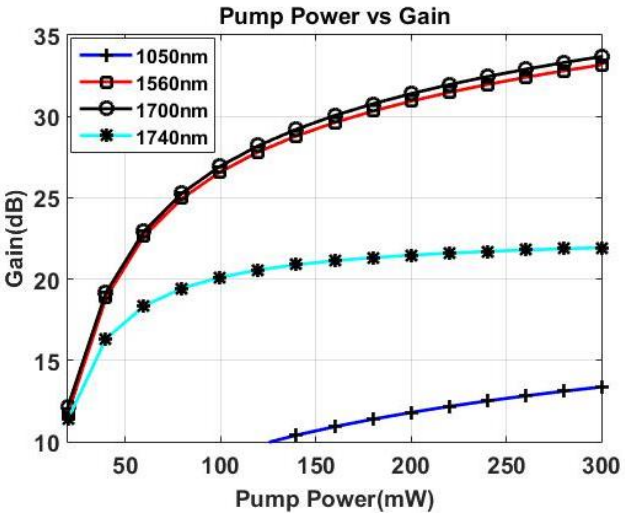

Fig. 12. Gain vs. Pump Power for doping concentration of 15.6×10^{24} m^{-3} numerical aperture of 0.3 (color online)

Fig. 13 shows the comparison of pumping cases when doping concentration of 40×10^{24} m^{-3} has been set when numerical aperture is 0.3. In this case, the response of 1560 nm, 1700 nm and 1740 nm pumping cases is almost the same, again the 1050 nm pump is found least efficient in this case. It can be observed that the gain of 1740 nm improves significantly by increasing doping concentration to 40×10^{24} m^{-3} from 15.6×10^{24} m^{-3}.

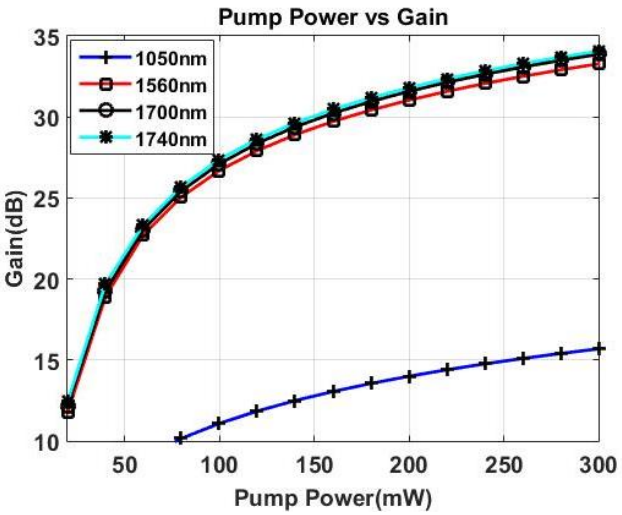

Fig. 13. Gain vs. Pump Power for doping concentration of 40×10^{24} m^{-3} numerical aperture of 0.3 (color online)

Fig. 14 and Fig. 15 show the gain variation for the considered pump cases when doping concentration is set to 15.6×10^{24} m^{-3} and 40×10^{24} m^{-3} respectively when the numerical aperture is 0.4. By comparing Fig. 12 and Fig. 14 it can be stated that if the available pump is 1740 mn then TDFA with the numerical aperture of 0.4 provides significant gain enhancement. The 1700 nm is the most efficient pumping, the pump of 1560 nm also provides good efficiency in this case.

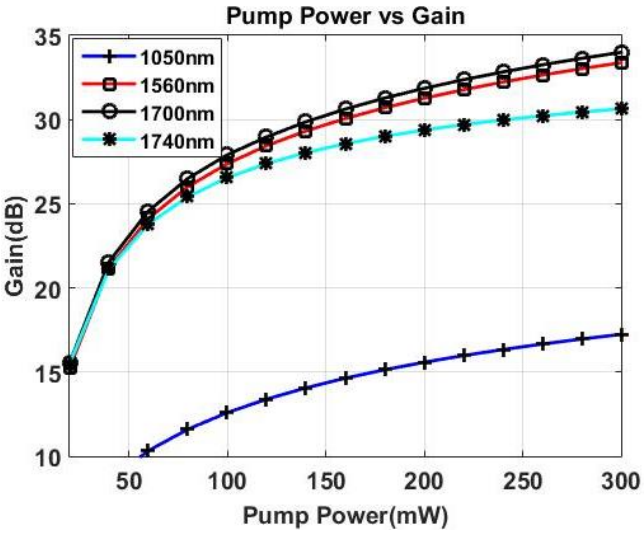

Fig. 14. Gain vs. Pump Power for doping concentration of 15.6×10^{24} m^{-3} numerical aperture of 0.4

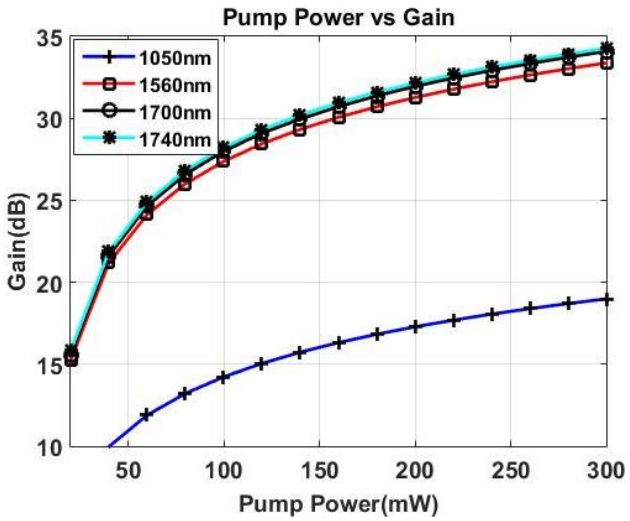

Fig. 15. Gain vs. Pump Power for doping concentration of 40×10^{24} m^{-3} Numerical aperture of 0.4 (color online)

F. Comparison with Similar Works

Muhammad Syauqi Kusyairi bin Jamalus et al. presented the TDFA optical amplifier for signals ranging from 1975 nm to 2000 nm. They proposed a double pass dual-stage TDFA configuration which achieved a maximum gain of 19.85 dB with 200 mW pump power of 1550 nm [13]. However, the double pass TDFA amplifier configuration is complex in construction therefore it is not a cost-effective approach. In the present work, only single-pass TDFA is presented which is cost-effective. In a similar demonstration Robert E. Tench et al. used a pump of 1567 nm, very high pump powers of 3.2W and 3.6W were used in the first state and the second state of TDFA respectively. They reported an internal small signal gain as high as 60.4 dB. The very high pump power makes the system unreliable and impractical as in long term the life of splices depends on the pump power used [14]. In the present work maximum pump power is restricted to 300 mW which makes the present work practical and attractive. M. A. Khamis et.al presented the TDFA for 2 µm application where they compared the pumps of 1570 nm and 793 nm. For the 500 mW pump power, they obtained the gain values of 30dB for the 1570 nm pump and 22dB for the 793 nm pump [15]. In the present work, the gain exceeding 30 dB has been obtained for a maximum pump power of 300 mW. It has been observed that the use of a 1740 nm pump with the selected doping concentration of 40×10^{24} m^{-3} and numerical aperture of 0.4 gives the maximum peak gain of 34.34dB for 300 mW pump power.

4. Conclusion

In this paper, the dependence of peak gain of TDFA on various factors has been investigated. Here, four pumps of wavelength 1050 nm, 1560 nm, 1700 nm, 1740 nm have been considered. The numerical aperture value of 0.3 and 0.4 are considered for every pumping case. Also, ion density values of 15.6×10^{24} m^{-3}, 20×10^{24} m^{-3}, 30×10^{24} m^{-3}, 40×10^{24} m^{-3} have been used for every pumping case. The pump power is varied from 20 mW - 300 mW. In this way, eight cases for each pump are considered and the gain vs pump power graphs have been plotted to check the dependence of peak gain of silica-based TDFA on the considered parameters. It has been observed that the peak gain is obtained at 1830 nm wavelength in each case. For pump power 300 mW, the maximum peak gain provided by the 1050 nm pump is 19.40dB. In the case of the 1560 nm pump, it is 33.40 dB. For 1700 nm pump wavelength it comes out to be 34.09 dB. For the 300 mW pump power, 1740 nm pump gives the maximum peak gain of 34.34dB. So, among all the 32 cases best peak gain (34.34dB) is given by the pump of 1740 nm for NA=0.4 and ion density of 40×10^{24} m^{-3}. In conclusion, it can be stated that if 1740 nm pumping is to be used then the TDFA with 0.4 numerical aperture should be used, otherwise for the TDFA with 0.3 numerical aperture a high doping concentration should be chosen. Also, it is observed that the 1050 nm pumping is very inefficient for the 2 µm region amplification. The performance of 1560 nm or 1700 nm pumping techniques is not dependent much on the numerical aperture, in both these cases, the doping concentration variation also does not affect the gain of TDFA.

References

[1] Z. Li, A. M. Heidt, J. M. O. Daniel, Y. Jung, S. U. Alam, D. J. Richardson, Optics Express **21**(8), 9289 (2013).
[2] S. Singh, R. S. Kaler, Optical Engineering **54**(10), 100901 (2015).
[3] M. A. Khamis, K. Ennser, Optics Communications **384**(1), 89 (2017).
[4] M. A. Khamis, K. Ennser, Journal of Lightwave Technology **34**(24), 5675 (2016).
[5] S. D. Emami, M. M. Dashtabi, H. J. Lee, A. S. Arabanian, H. A. A. Rashid, Scientific Reports **7**(1), 12747 (2017).
[6] P. Peterka, I. Kasik, V. Matejeca, W. Blanc, B. Faure, B. Dussardier, G. Monnom, V. Kubecek, Optical Materials **30**(1), 174 (2007).
[7] R. Singh, M. L. Singh, B. Kaur, Optik **123**(20), 1815 (2012).
[8] R. Singh, M. L. Singh, Journal of Optical Technology **88**(4), 215 (2021).
[9] R. Singh, M. L. Singh, Optik **127**(2), 876 (2016).
[10] P. Peterka, B. Faure, W. Blanc, M. Karasek, B. Dussardier, Optical and Quantum Electronics **36**, 201 (2004).
[11] R. Singh, M. L. Singh, International Conference on Recent Advances and Innovations in Engineering, ICRAIE, December 23-25, Jaipur, India, 5 (2016).
[12] M. M. Kozak, R. Caspary, W. Kowalsky, Proceedings of 2004 6th International Conference on Transparent Optical Networks, Wroclaw, Poland, 51 (2004).

[13] Muhammad Syauqi Kusyairi bin Jamalus, Nelidya Md. Yusoff, Abdul Hadi Sulaiman, Indonesian Journal of Electrical Engineering and Computer Science **15**(3), 1203 (2019).

[14] Robert E. Tench, Clement Romano, Jean-Marc Delavaux, Applied Optics **57**(21), 5948 (2018).

[15] M. A. Khamis, K. Ennser, Journal of Lightwave Technology **34**(24), 5675 (2016).

*Corresponding author: rajandeep.ece@gndu.ac.in